

Single Molecule Characterization of P-selectin/Ligand Binding^{*S}

Received for publication, December 27, 2002, and in revised form, January 8, 2003
Published, JBC Papers in Press, January 8, 2003, DOI 10.1074/jbc.M213233200

William Hanley^{‡§}, Owen McCarty^{‡§}, Sameer Jadhav[‡], Yiider Tseng[‡], Denis Wirtz^{‡¶||},
and Konstantinos Konstantopoulos^{‡||**}

From the [‡]Department of Chemical and Biomolecular Engineering, ^{**}Department of Biomedical Engineering, and
[¶]Molecular Biophysics Program, The Johns Hopkins University, Baltimore, Maryland 21218

P-selectin expressed on activated platelets and vascular endothelium mediates adhesive interactions to polymorphonuclear leukocytes (PMNs) and colon carcinomas critical to the processes of inflammation and blood-borne metastasis, respectively. How the overall adhesiveness (*i.e.* the avidity) of receptor/ligand interactions is controlled by the affinity of the individual receptors to single ligands is not well understood. Using single molecule force spectroscopy, we probed *in situ* both the tensile strength and off-rate of single P-selectin molecules binding to single ligands on intact human PMNs and metastatic colon carcinomas and compared them to the overall avidity of these cells for P-selectin substrates. The use of intact cells rather than purified proteins ensures the proper orientation and preserves post-translational modifications of the P-selectin ligands. The P-selectin/PSGL-1 interaction on PMNs was able to withstand forces up to 175 pN and had an unstressed off-rate of 0.20 s⁻¹. The tensile strength of P-selectin binding to a novel O-linked, sialylated protease-sensitive ligand on LS174T colon carcinomas approached 125 pN, whereas the unstressed off-rate was 2.78 s⁻¹. Monte Carlo simulations of receptor/ligand bond rupture under constant loading rate for both P-selectin/PSGL-1 and P-selectin/LS174T ligand binding give distributions and mean rupture forces that are in accord with experimental data. The pronounced differences in the affinity for P-selectin/ligand binding provide a mechanistic basis for the differential abilities of PMNs and carcinomas to roll on P-selectin substrates under blood flow conditions and underline the requirement for single molecule affinity measurements.

Cellular adhesion mediated by biological macromolecules and their respective ligands plays an essential role in a number of diverse biological phenomena including inflammation and cancer metastasis. Leukocyte recruitment to sites of infection is regulated by highly specific receptor/ligand interactions that allow leukocytes to first tether and roll on activated endothelium under hydrodynamic shear and then firmly adhere prior to extravasation into the tissue space. These stages are mediated via three distinct classes of adhesion molecules: the selec-

tins, integrins, and immunoglobulins (1–3). Accumulating evidence suggests that tumor cell arrest in the microcirculation is also mediated through receptor/ligand interactions between tumor cells and the vascular endothelium in a manner analogous to leukocyte recruitment (4–6). Both processes involve highly regulated molecular events that rely on the local circulatory hemodynamics and the mechanical and kinetic properties of participating adhesive molecular groups, which have yet to be characterized at the single molecule level.

The involvement of P-selectin is critical within immune system functioning. P-selectin, a cell-surface glycoprotein expressed on activated endothelial cells and platelets, supports leukocyte tethering and rolling in response to inflammatory signals by interacting with its counter-receptor, P-selectin glycoprotein ligand-1 (PSGL-1),¹ located on leukocyte microvilli (7). Recently, specific P-selectin-tumor cell interactions have been revealed providing direct evidence of its participation in metastasis as well. The most compelling evidence for the role of P-selectin in the metastatic process is the pronounced inhibition of metastasis in P-selectin-deficient mice compared with wild-type controls in a colon carcinoma cell model (8, 9). Several lines of evidence suggest that the P-selectin ligands on a variety of tumor cell lines are sialylated molecules distinct from PSGL-1 (10–12). Along these lines, enzymatic removal of these PSGL-1 distinct P-selectin ligands from the carcinomas results in a marked reduction of experimental metastasis (9).

Biophysical parameters of P-selectin/ligand binding have previously been obtained by quantifying leukocyte tethering duration (13, 14) and rolling velocity (15) on purified P-selectin substrates. These techniques may not effectively differentiate avidity from the affinity of a single receptor/ligand pair and, most importantly, rely on broad assumptions to estimate the forces on receptor/ligand bonds. Previous single molecule work on the characterization of P-selectin/PSGL-1 binding was performed using purified adhesion molecules rather than intact target cells (16). However, subtle differences between native and recombinant forms of PSGL-1 (17) can impact biophysical measurements. Here we employ single molecule force spectroscopy to probe the tensile strength and unstressed off-rate of P-selectin/PSGL-1 binding on intact human polymorphonuclear leukocytes (PMNs), a technique that preserves the orientation and post-translational modifications of PSGL-1. This methodology was extended to characterize P-selectin/ligand binding on intact metastatic colon carcinoma cells. Macroscopic studies performed using a parallel-plate flow chamber reveal that PSGL-1-mediated PMN recruitment to P-selectin sub-

^{*} This work was supported by a Whitaker Foundation grant and National Science Foundation Grant CTS0210718. The costs of publication of this article were defrayed in part by the payment of page charges. This article must therefore be hereby marked “advertisement” in accordance with 18 U.S.C. Section 1734 solely to indicate this fact.

^S The on-line version of this article (available at <http://www.jbc.org>) contains Supplemental Fig. 1.

[§] Both authors contributed equally to this work.

^{||} To whom correspondence may be addressed. Dept. of Chemical and Biomolecular Engineering, The Johns Hopkins University, 3400 N. Charles St., Baltimore, MD 21218. Tel.: 410-516-6290; Fax: 410-516-5510; E-mail: kkonsta1@jhu.edu (K. K.) or Tel.: 410-516-7006; Fax: 410-516-5510; E-mail: wirtz@jhu.edu (D. W.).

¹ The abbreviations used are: PSGL-1, P-selectin glycoprotein ligand-1; D-PBS, D-phosphate-buffered saline; BSA, bovine serum albumin; benzyl-GalNAc, benzyl-2-acetamido-2-deoxy- α -D-galactopyranoside; mAb, monoclonal antibody; DMJ, deoxymannojirimycin; threo-PPPP, D,L-threo-1-phenyl-2-amino-3-morpholino-1-propanol hydrochloride; PMN, polymorphonuclear leukocyte; MFP, molecular force probe; RT, room temperature; ANOVA, analysis of variance.

strates is more efficient than tumor cell-P-selectin interactions under dynamic flow conditions and results in stable *versus* transient rolling interactions (10–12). Therefore, we aimed to provide a mechanistic interpretation at the molecular level for the differential abilities of PMNs and tumor cells to roll on P-selectin by evaluating and comparing the affinity of single P-selectin/ligand bonds. The LS174T human colon adenocarcinoma cell line was chosen as a model because it has been used in a number of diverse assays ranging from characterization of surface adhesion molecules to cell-substrate and cell-cell interaction studies (5, 10, 18, 19). Finally, using highly specific enzymes and glycoconjugate biosynthesis inhibitors, we have characterized the biochemical nature of the putative P-selectin ligand on LS174T colon carcinomas.

MATERIALS AND METHODS

Reagents—The chimeric form of P-selectin-IgG Fc (P-selectin) consisting of the lectin, epidermal growth factor, and nine consensus repeat domains for human P-selectin linked to each arm of human IgG1 was a generous gift from Dr. Ray Camphausen of Wyeth External Research (Cambridge, MA) (20). All of the other reagents were purchased from Sigma unless otherwise stated.

Cell Culture—LS174T human colon adenocarcinoma cells were obtained from the American Type Culture Collection (Manassas, VA) and cultured in the recommended medium. Cells were detached from culture flasks using 0.25% trypsin, EDTA for 2 min at 37 °C (5, 10, 21, 22). For force spectroscopy experiments, 20 μ l of 1×10^7 cells/ml LS174T cell suspension was layered on 35-mm tissue culture dishes and subsequently incubated overnight at 37 °C to allow adhesion to the culture dish and regeneration of surface glycoproteins (5, 10). This procedure resulted in ~20% cellular confluency as assessed by phase-contrast microscopy. Prior to use in force spectroscopy experiments, non-adherent LS174T cells were removed by gentle rinsing with D-PBS, and the standard medium was replaced with serum-free medium containing Hank's salts, which help to stabilize the pH outside of the 5% CO₂ environment of an incubator. In flow-based adhesion assays, the trypsinized LS174T cell suspension was incubated for 2 h at 37 °C to regenerate surface glycoproteins and was used immediately thereafter (5, 10, 21, 22).

Cell Treatments—In selected experiments, LS174T cell suspensions were incubated for 30 min at 37 °C with 20 μ g/ml trypsin to cleave cell surface glycoproteins (21) and washed once before use in flow-based assays. For metabolic inhibitor studies, LS174T cells were cultured for 48 h at 37 °C in medium containing either 2 mM benzyl-2-acetamido-2-deoxy- α -D-galactopyranoside (benzyl-GalNAc) to inhibit O-linked glycosylation (21) or 1 mM deoxymannojirimycin (DMJ) to disrupt N-linked processing (21), or for 96 h, LS174T cells were cultured with 5 μ M D,L-threo-1-phenyl-2-amino-3-morpholino-1-propanol hydrochloride (threo-PPPP, Matreya, Inc., State College, PA), which blocks the transfer of UDP-glucose to ceramide, thereby blocking the synthesis of glycosphingolipids having a glucosylceramide core (21). Treated LS174T cells were washed twice before use in experiments, and cell viability was consistently >97% as detected by the trypan blue exclusion assay.

PMN Isolation and Monolayer—Human PMNs were isolated from citrate phosphate dextrose-anticoagulated venous blood of healthy volunteers as described previously (21, 22), resuspended at 1×10^6 cells/ml in Ca²⁺/Mg²⁺-free D-PBS (0.1% BSA), and stored at 4 °C for no more than 3 h before use in all experiments. To immobilize PMNs, 200 μ l of the isolated PMN cell suspension was allowed to incubate on a 35-mm tissue culture dish for 5 min at RT (23). To prevent further activation, a 1% formalin-D-PBS solution was added to the cell culture dish and maintained at RT for 10 min (23). The PMN monolayer was rinsed and refilled with D-PBS containing Ca²⁺/Mg²⁺. This procedure resulted in a PMN monolayer of ~40% confluency.

Cantilever Functionalization—To provide a surface that readily binds soluble proteins, molecular force probe (MFP) cantilevers (TM Microscopes, Sunnyvale, CA) were silanized with 2% 3-aminopropyltriethoxysilane (10). The cantilevers were then incubated in a 3.3- μ g/ml solution of anti-human IgG Fc mAb in D-PBS containing 50-fold molar excess of the cross-linker bis(sulfosuccinimidyl) suberate (BS³, Pierce) for 30 min followed by quenching with Tris buffer. Cantilevers were subsequently incubated with dilute P-selectin-IgG Fc chimera protein in D-PBS for 2 h at RT followed by immersion in 1% BSA to block nonspecific interactions. Binding the IgG Fc portion of the P-selectin chimera to the immobilized anti-IgG Fc mAb on the cantilever main-

tains its proper functional orientation. Concentrations of the anti-human IgG Fc and P-selectin chimera solutions were optimized to result in a low percentage of binding events during force spectroscopy experiments (~30 binding events/100 cell contacts). 1.8 and 3.0 μ g/ml P-selectin-IgG Fc solutions were used for PMN and LS174T cell experiments, respectively.

Single Molecule Force Spectroscopy—Experiments were conducted using an MFP (Asylum Research Inc., Santa Barbara, CA). Two triangular-shaped cantilevers with nominal spring constants of 10 and 40 piconewton/nm were calibrated using thermal noise amplitude, and their deflection was measured by laser reflection onto a split photodetector. Measurements were carried out using serum-free medium for the LS174T cells or D-PBS containing Ca²⁺/Mg²⁺ for PMNs. The 35-mm culture dish containing the adherent cellular monolayer immersed in either medium or D-PBS was placed on the MFP stage and positioned so that the cantilever was directly above a single cell. The distance between the cantilever and the cell was adjusted so that each approach cycle resulted in a slight depression force on the cell before reproach. The reproach velocity was varied from 0.5 to 30 μ m/s, and the dwell time between the cantilever and the cell was set to 0.001 s to minimize the occurrence of multiple events (24). Rupture forces were derived from force *versus* distance traces using IgorPro 3.11 software (Wavemetrics, Inc., Lake Oswego, OR). Histograms representing ~350 approach/reproach cycles were compiled for each reproach velocity, and the mean rupture force of a P-selectin/ligand interaction was evaluated. Prior work has shown that the mean and the mode of the rupture force approach one another over the higher loading rate regime, and the mean can accurately be used to estimate Bell model parameters (25).

Flow Cytometry—Expression levels of the P-selectin ligand on LS174T cells and human PMNs were quantified by indirect single color immunofluorescence and flow cytometry. To this end, P-selectin chimera solution was preincubated with fluorescein isothiocyanate-labeled goat anti-human IgG Fc mAb for 1 h at RT before incubation of the mixture with either LS174T or PMN cell suspensions at 1×10^6 cells/ml in D-PBS, 0.1% BSA (8). After incubation at 4 °C for 1 h, cells were washed with D-PBS and then fixed using 2% formalin (v/v) (8). Cells were washed again and resuspended in D-PBS containing 0.1% BSA. Background levels were determined by incubating with conjugated protein in the presence of 30 mM EDTA (8).

Flow-based Adhesion Assays—P-selectin-coated surfaces were prepared by incubating 1–4 μ g/ml anti-human IgG Fc mAb in D-PBS on untreated 35-mm polystyrene culture dishes overnight at 4 °C. Equally diluted solutions of P-selectin-IgG Fc protein were then layered on the dish and allowed to incubate for 2 h at RT before rinsing with D-PBS and blocking with 1% BSA for 2 h (10). Suspensions of either LS174T cells or PMNs at a final concentration of 1×10^6 cells/ml were perfused over the P-selectin-coated dishes using a parallel-plate flow chamber (250- μ m-channel depth, 5.0-mm-channel width) for 3 min at 37 °C (26). Rolling velocities were computed as the distance traveled by the centroid of the translating cell divided by the time interval (10, 26).

Statistical Analysis—Data are expressed as the mean \pm S.E. for at least three independent experiments. Statistical significance of differences between the means was determined by ANOVA. Whether the means were shown to be significantly different ($p < 0.05$), multiple comparisons were performed by the Tukey test.

RESULTS

Single Molecule Force Spectroscopy Measurements—An MFP was used to determine the tensile strength and unstressed off-rate of P-selectin binding to its ligands on intact human PMNs and LS174T colon carcinomas at the single molecule level. To this end, force-distance traces (Fig. 2a) were generated by lowering the P-selectin-functionalized cantilever to the immobilized cellular monolayer (Fig. 1), maintaining P-selectin/cell contact for a set period of time (0.001 s) to allow establishment of receptor/ligand binding and subsequently retracting the cantilever from the cell surface at a constant prescribed velocity. Upon retraction of the cantilever, the force was recorded as a function of the vertical displacement until dissociation of P-selectin/ligand bonds occurred (Fig. 2a). Under the conditions of this study, receptor/ligand unbinding at any given reproach velocity predominantly involved single rather than multiple steps (24) as shown in the representative force-distance trace. Additionally, rupture force histograms at a given reproach velocity always indicated a single peak distribution

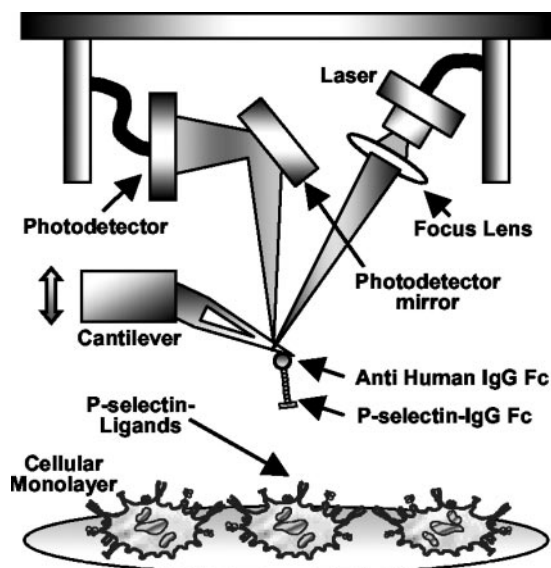


FIG. 1. MFP schematic indicating the use of intact cells to measure *in situ* cellular adhesion forces. The cantilever was positioned directly above a cell and was allowed to approach until it touched and slightly deformed the cell membrane before reapproaching at a set velocity. This approach/reapproach cycle was repeated hundreds of times to obtain a statistically significant value for the P-selectin/ligand rupture force at that velocity.

for both LS174T cell and PMN experiments (Fig. 2b), suggesting the rupture of a single P-selectin/ligand complex (24). A single peak distribution also indicates that nonspecific interactions did not play a significant role in these measurements.

To ensure that most binding events were mediated by a single receptor/ligand pair, a low frequency of binding events (an average of 30 per 100 contacts) was achieved by decorating cantilevers with sufficiently dilute P-selectin chimera solutions. The concentration of P-selectin on the cantilever was greater for the LS174T cell (3 $\mu\text{g}/\text{ml}$) versus PMN (1.8 $\mu\text{g}/\text{ml}$) experiments, a result of the differing expression levels of P-selectin ligands on the cell surfaces (Table I). The percentage of binding events in this study ranged from 18 to 40% with 30% being the targeted average value for both PMN and LS174T cells. Based on Poisson distribution statistics, when 30% of cantilever to cell contacts lead to P-selectin/ligand binding, 83% of those successful adhesions are probably because of a single bond ($N_b = 1$) (25, 27). Moreover, statistics predict that there will be 15% double bonds ($N_b = 2$) and <3% will have $N_b > 2$.

Two different control experiments were performed to demonstrate the specificity of P-selectin/ligand binding. First, the addition of EDTA to the tissue culture dish at a final concentration of 0.5 mM consistently abrogated binding (Fig. 2a), a finding that is in accord with the calcium dependence of selectin/ligand binding (7, 10). Second, incubating the P-selectin-coated cantilever with a function-blocking anti-P-selectin mAb AK4 (50 $\mu\text{g}/\text{ml}$, BD Biosciences) drastically reduced the frequency of binding events from ~30% to <5% (Fig. 2a), an observation that is consistent with other receptor/ligand measurements at the single molecule level blocked by mAbs (25, 28). These observations were valid for both LS174T and PMN cells.

Calculation of Bell Model Parameters and Monte Carlo Analysis—To construct a plot of rupture force versus loading rate, rupture forces and corresponding loading rates for hundreds of events were tabulated off-line and compiled into histograms for each reapproach velocity and mean rupture forces were calculated (25). Histograms from a representative P-selectin/PSGL-1 experiment over a range of reapproach velocities are presented in Fig. 2b. The loading rate (pN/s) for each reapproach

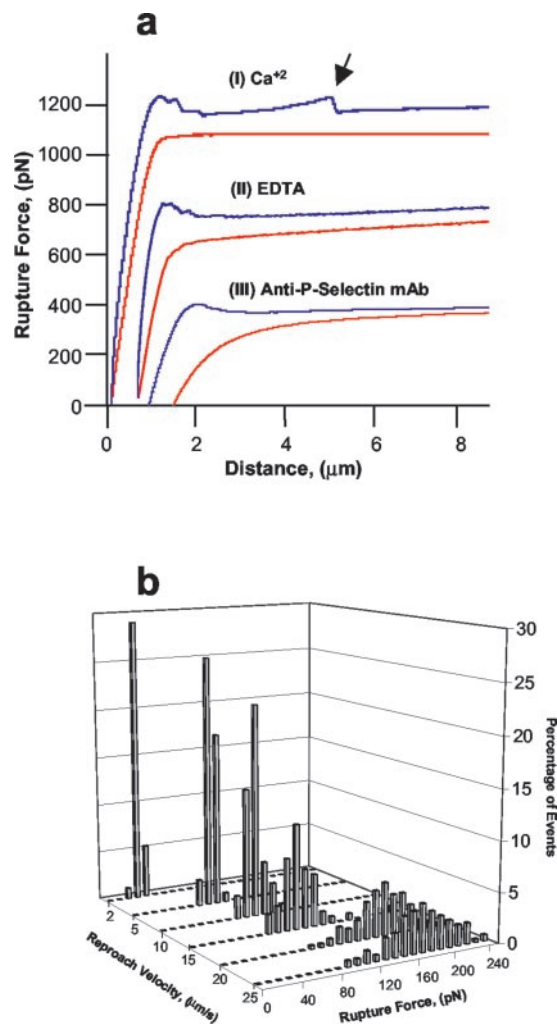


FIG. 2. *a*, force versus vertical displacement traces taken from an experiment using LS174T colon carcinomas in the absence (I) and presence of either EDTA (II) or blocking anti-P-selectin mAb (III). *b*, histograms of P-selectin to PSGL-1 binding on human PMNs at six different reapproach velocities representing at least 300 cell contacts at each velocity.

TABLE I
Expression levels of P-selectin ligands and average rolling velocities of PMNs and LS174T colon carcinomas on P-selectin substrates

Geometric mean fluorescence intensities are given for PMNs and LS174T colon carcinomas with background levels in parenthesis ($n = 4$) as assessed by indirect immunofluorescence coupled with flow cytometry. Rolling velocities of PMNs and LS174T colon carcinomas perfused over P-selectin substrates at a wall shear stress of 1 dyne/cm^2 . Values are the mean of 15–20 cells.

	Geometric mean fluorescence	Rolling velocity
		$\mu\text{m}/\text{s}$
PMN	830 ± 45 (7.0 ± 1.8)	8.0 ± 0.7
LS174T	280 ± 10 (6.3 ± 1.0)	110 ± 8.8

velocity was determined by first evaluating the slope of the force versus distance trace just before each rupture event (Fig. 2a) and multiplying this number (pN/ μm) by the reapproach velocity ($\mu\text{m}/\text{s}$). The Bell model parameters, namely the unstressed off-rate k_{off}^0 and the separation distance along the reaction coordinate x_β were tabulated (Table II) by a least squares fit to the linear region of the rupture force versus logarithm of loading rate and extrapolating to zero force (Fig. 3a) (25, 29, 30). At some lower limit of the loading rate, the force versus logarithm of loading rate plot begins to deviate

TABLE II
Bell model parameters for P-selectin/PSGL-1 and P-selectin/LS174T cell interactions

P-selectin ligand	Range, loading rate	x_β	k_{off}°
	pN/s	nm	s ⁻¹
PSGL-1	100–10,000	0.14	0.20
LS174T	200–5000	0.13	2.78
PSGL-1	All	0.12	0.19
LS174T	All	0.09	2.96

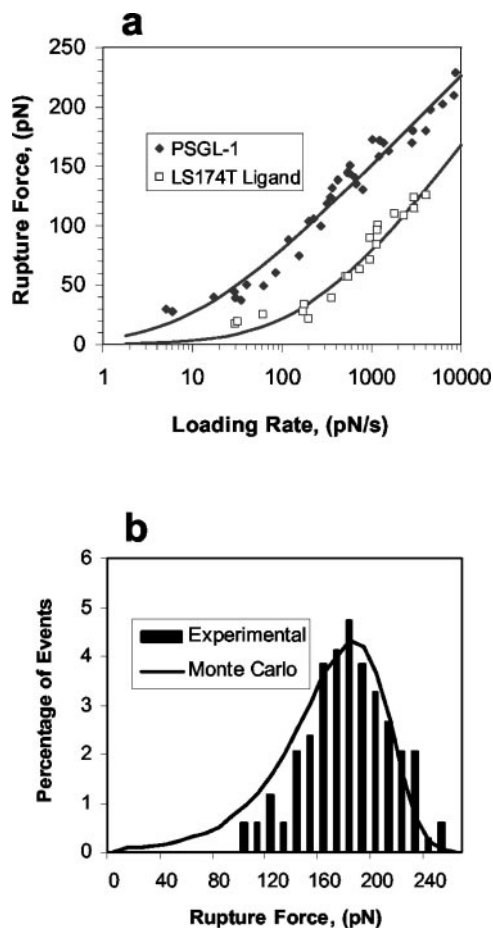


FIG. 3. *a*, molecular force versus loading rate for P-selectin binding to PMN/LS174T cells. The data shown comprise at least five independent experiments for each cell type conducted on separate days to validate reproducibility. The superimposed solid line indicates the non-linear least squares fit over the entire range of experimental loading rates found from the probability density function for bond rupture and corresponding Bell model parameters. *b*, Monte Carlo simulation for P-selectin/PSGL-1 binding at a reproach velocity of 25 $\mu\text{m/s}$.

from linearity or develop another linear region (25, 31). This phenomenon may indicate a change of unbinding mechanism and transition states at lower loading rates (29), but predictably the curve should approach the origin as zero loading rate provides zero force. This lower limit of linearity was reached at ~ 100 pN/s for P-selectin to PSGL-1 and 200 pN/s for P-selectin to the ligand on LS175T cells (Fig. 3*a*). Table II gives the values for k_{off}° and x_β for both cell types over the higher loading rate regions. As can be seen, the unstressed off-rate is dramatically higher for P-selectin/LS174T ligand (2.78 s^{-1}) than for P-selectin/PSGL-1 (0.20 s^{-1}), whereas the values for x_β are similar.

To validate the accuracy of the calculated Bell model parameters, the experimental data were modeled over the entire range of loading rates by using the probability density function for bond rupture (25, 31) as shown in Equation 1,

$$p(t, f) = k_{\text{off}}^\circ \exp\left(\frac{x_\beta r_f t}{k_b T}\right) \exp\left[-\frac{k_{\text{off}}^\circ k_b T}{r_f} \left(\exp\left(\frac{x_\beta r_f t}{k_b T}\right) - 1\right)\right] \quad (\text{Eq. 1})$$

where $p(t, f)$ is the probability of bond rupture at time t , r_f is the loading rate, k_b is the Boltzmann's constant, and T is the absolute temperature. The mean rupture force, $\langle f_b \rangle$, from this distribution (25, 31) is given by Equation 2.

$$f_b = \frac{k_b T}{x_\beta} \exp\left(\frac{k_{\text{off}}^\circ k_b T}{x_\beta r_f}\right) \int_0^\infty \frac{\exp\left(\frac{k_{\text{off}}^\circ k_b T}{x_\beta r_f} \frac{t}{\tau}\right)}{t} dt \quad (\text{Eq. 2})$$

The Bell model parameters, k_{off}° and x_β , were estimated by a non-linear least squares fit of the above equation to the experimental data over the entire range of loading rates (Fig. 3*a*). As shown in Table II, the values of Bell model parameters obtained by the non-linear fit are in good agreement with those obtained by the linear fit of rupture force versus logarithm of loading rate over the high loading rates regime.

To further validate the agreement of our data with the Bell model, Monte Carlo simulations of receptor/ligand bond rupture under constant loading rates were performed. Given a k_{off}° and x_β in each simulation, we calculated the rupture force ($F_{\text{rup}} = r_f \times n\Delta t$) for which the probability of bond rupture P_{rup} is greater than P_{ran} , a random number between zero and one,

$$P_{\text{rup}} = 1 - \exp\left[-k_{\text{off}}^\circ \exp\left(\frac{x_\beta r_f n\Delta t}{k_b T}\right) \Delta t\right] \quad (\text{Eq. 3})$$

where Δt is the interval and $n\Delta t$ is the time step. The distributions and means of rupture forces obtained in our experiments are in accord with these simulations as shown for a representative experimental condition and Monte Carlo simulations for P-selectin/PSGL-1 binding at a retract velocity of 25 $\mu\text{m/s}$ (Fig. 3*b*).

Taken together, our data indicate that the tensile strength of P-selectin binding to its ligand on LS174T colon carcinoma is significantly lower than that of P-selectin/PSGL-1 binding at any given loading rate (Fig. 3*a*). The differences in their respective tensile strengths as well as the unstressed off-rates and ligand densities provide a mechanistic basis for the differential rolling behavior of LS174T colon carcinomas and PMNs on P-selectin substrates observed in flow-chamber experiments (Table I).

Biochemical Characterization of P-selectin Ligands on LS174T Colon Carcinomas—We have recently shown that the P-selectin ligand on LS174T colon carcinomas is a novel sialylated molecule functionally distinct from the previously identified P-selectin ligands PSGL-1, glycoprotein Ib/IX, and CD24 (10). Further experiments on the biochemical nature of the target ligand on LS174T cells reveal that it is a protease-sensitive glycoprotein rather than a glycosphingolipid (Fig. 4*a*). This was demonstrated by the marked inhibition of trypsin-treated LS174T cells to tether to purified P-selectin as opposed to cells cultured in the presence of a glycosphingolipid biosynthesis inhibitor threo-PPPP (21), which retained their ability to bind to P-selectin underflow (Fig. 4*a*).

We next examined whether critical P-selectin binding determinants on LS174T colon carcinoma cells are presented on O-linked and/or N-linked glycans. To this end, LS174T cells were cultured in the presence of either benzyl-GalNAc known to inhibit O-linked glycosylation or DMJ (which disrupts N-linked processing) before use in adhesion assays. The results indicated that LS174T cell tethering to P-selectin-coated surfaces was drastically inhibited by benzyl-GalNAc but not by DMJ (Fig. 4*a*). Similar results were obtained using single molecule force spectroscopy. More specifically, the treatment of

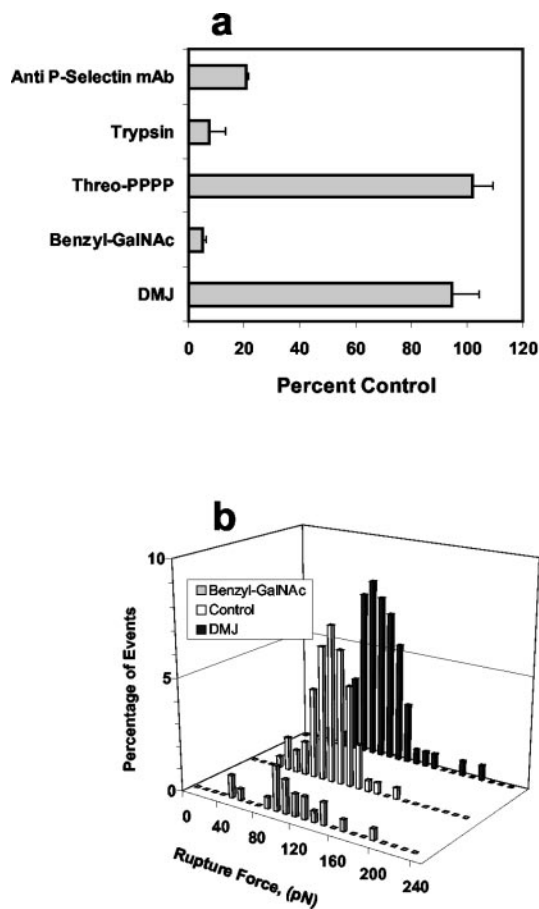


FIG. 4. *a*, LS174T cell tethering/rolling over purified P-selectin at a wall shear stress of 1 dyne/cm². Data are expressed as the percentage of untreated (control) LS174T cells that interacted with purified P-selectin throughout the 3-min experiment. Immobilized P-selectin was incubated with an anti-P-selectin mAb (AK4, 20 μ g/ml) for 10 min prior to LS174T cell perfusion. LS174T cells were incubated with trypsin (20 μ g/ml) for 1 h at 37 $^{\circ}$ C. Alternatively, untreated cells were cultured with threo-PPPP (5 μ M) or benzyl-GalNAc (2 mM), an *O*-linked glycan extension inhibitor, or DMJ (1 mM), an *N*-linked glycan extension inhibitor. *b*, P-selectin binding to LS174T tumor cells as measured by single molecule force spectroscopy. Shown are rupture force histograms for control LS14T cells and cells cultured in media containing benzyl-GalNAc and DMJ.

LS174T cells with benzyl-GalNAc reduced the frequency of binding from 32 to <8%, whereas DMJ impacted neither the force distribution nor the frequency of events (Fig. 4b). Collectively, these data reveal that the P-selectin ligand is a novel *O*-linked, sialylated protease-sensitive structure and does not require *N*-glycans for binding.

The interaction of PSGL-1 with the actin cytoskeleton is known to regulate the strength of leukocyte adhesion to P-selectin as evidenced by increased resistance to shear-induced detachment forces upon PMN treatment with cytochalasin B, a compound that caps the growing end of actin filament (32). Therefore, we wished to examine whether P-selectin-mediated LS174T binding is also dependent on actin cytoskeleton. However, the treatment of LS174T cells with cytochalasin B affected neither the extent nor the pattern of cell tethering to immobilized P-selectin chimera at a wall shear stress of 1 dyne/cm² (data not shown). Furthermore, latrunculin A (1 μ M), a compound that prevents actin polymerization by irreversibly binding to actin monomers (33), failed to affect P-selectin-mediated LS174T cell adhesion (data not shown), although it nearly abrogated PMN binding to P-selectin under flow (control samples (156 \pm 15 tethered PMNs/mm²) versus lantrinculin-

treated samples (7 \pm 1 PMNs/mm²)). Cumulatively, these data provide evidence for the absence of actin cytoskeleton involvement in the regulation of P-selectin/LS174T P-selectin ligand interactions unlike P-selectin/PSGL-1 (32).

DISCUSSION

Using single molecule force spectroscopy, we measured the biophysical parameters of P-selectin binding to ligands on intact LS174T colon carcinomas and PMNs at a single molecule resolution. By carefully controlling the concentration and orientation of immobilized P-selectin chimeras on the surface of an MFP cantilever and regulating its contact time and depression force on the immobilized cells, we evaluated the affinity of single P-selectin/ligand interactions under conditions that preserve all appropriate post-translational ligand modifications. In this study, we determined that the tensile strength of P-selectin/PSGL-1 binding is substantially greater than P-selectin/LS174T P-selectin ligand binding for all loading rates. Additionally, the unstressed off-rate for P-selectin/PSGL-1 (0.20 s⁻¹) was significantly different from the value for P-selectin/ligand on LS174T cells (2.78 s⁻¹). Thus, the differential avidity of PMNs and LS174T colon carcinomas for P-selectin substrates as assessed by rolling assays is attributed in part to intrinsic differences in receptor/ligand binding affinity as well as varying densities of ligands on their respective cell surfaces.

The kinetics of P-selectin to PSGL-1 binding has previously been studied by several different techniques including neutrophil tethering lifetime as assessed in flow-chamber experiments (13, 14, 34), plasmon resonance (35), and atomic force microscopy (16). To extract the biophysical parameters (tensile strength and unstressed off-rate) from neutrophil tethering measurements, several assumptions are required. First, the rolling cell is assumed to be a rigid sphere decorated with immobile adhesion molecules. However, leukocytes are covered with deformable microvilli where cellular adhesion molecules are concentrated, and experiments confirm that their rolling velocity over P-selectin substrates is greatly influenced by the processes of microvilli elongation and cytoskeletal rearrangement (15). Additionally, the applied force on a receptor/ligand bond is estimated from the wall shear stress and approximate geometric relationships (13, 15), because the actual force exerted on the receptor/ligand pair is unknown. Here, we have experimentally measured each bond rupture force and rigorously determined its respective loading rate by evaluating the slope of the force-distance trace just before the rupture event.

The highest value for a P-selectin/PSGL-1 rupture force that we determined approached 175 pN, a value similar to that found by Fritz *et al.* (16) using single molecule force spectroscopy, although our results were obtained at substantially higher re-proach velocities. The relative loading rates for the two studies, which would allow direct comparisons to be made, are unknown. The unstressed off-rate for P-selectin/PSGL-1 calculated in this study was 0.20 s⁻¹, a result that lies in between the value obtained by Fritz *et al.* (0.02 s⁻¹) (16) and the studies using flow-chambers (\sim 1 s⁻¹) (13, 14, 34). Differences between our Bell Model parameters for P-selectin/PSGL-1 and those calculated by Fritz *et al.* (16) may originate from slight differences between the recombinant form of PSGL-1 and the natural form on PMNs or any molecular orientation modifications that occur when PSGL-1 is nonspecifically immobilized. Interestingly, if the Bell model parameters are found by fitting a line to the low loading rate regime (up to 100 pN/s), the off-rate at 0.03 s⁻¹ approaches that by Fritz *et al.* (16). However, we have chosen to calculate the Bell model parameters from a linear fit to data within the higher loading rate regime (100–10000 pN/s), a decision also made by others using single molecule-spectroscopic techniques (25). Using a Monte Carlo simulation, Tees *et al.* (25) concluded that for

selectin-carbohydrate binding, values for Bell model parameters are correctly estimated from the steeper, higher loading rate region. The lower loading rate regime does not in fact represent another set of parameters but is consistent with a single model spanning low to intermediate loading rates. In addition, estimations for the physiological loading rates exerted on cellular adhesion molecules range from ~ 100 – 10000 pN/s (25). It is noteworthy that the Bell model parameters calculated using Equation 2 spanning the entire range of loading rates showed excellent agreement with those obtained from linear fit at the high loading rate regime. Furthermore, Monte Carlo simulations using these parameter values yield rupture force distributions in accord with those observed experimentally.

The impact of undesirable multiple events during single molecule force spectroscopy has been evaluated using Monte Carlo simulations (25). At 30% binding/cell/cantilever contact, it is possible that 17% approach/reproach cycles may involve multiple adhesions, which may impact the lifetime of bound complexes and inflate rupture force values. However, it has been found that multiple events only very modestly reduce the theoretically attainable Bell model parameters found from simulations that involve strictly single events (25). In the case of 40% binding, which means that 23% multiple bonds are expected, the k_{off}^* and x_{β} parameters were reduced by only 7 and 3%, respectively (25).

To effectively use PMNs in an MFP experiment, PMNs must be firmly immobilized on a substrate and subsequently fixed to prevent further morphological changes (23). The fixation of PMNs has been shown to abrogate microvillus elasticity, causing them to behave as PSGL-1-coated rigid microbeads but without impairing the molecular interaction between P-selectin and PSGL-1 (15). The process of fixing PMNs decreases the likelihood that the applied load on the P-selectin/PSGL-1 complex will be partially dissipated by viscous deformation during microvilli extension. Thus, the rupture forces for fixed PMNs may be higher at all loading rates than for unfixed PMNs, because nearly the entire applied load is placed on the receptor/ligand pair and any cytoskeletal contributions have been eliminated.

We also examined the effects of fixation with 1% formalin on the biophysical parameters of P-selectin/ligand binding on LS174T cells. Our experiments reveal that neither the tensile strength at all loading rates nor the Bell model parameters were appreciably impaired by the fixation process (see Supplemental Fig. 1), a finding that may be partially attributed to the lack of actin cytoskeleton interaction with P-selectin ligand on LS174T cells. Thus, under experimental conditions, in which orientation and post-translational modifications of P-selectin ligands are preserved and the cytoskeletal contributions have been minimized in both cell types, the tensile strength and affinity of P-selectin/PSGL-1 interactions are higher than those of P-selectin/LS174T selectin ligand binding. Although we have not identified the putative P-selectin ligand on the LS174T cell surface, our data indicate that it is a novel sialylated, protease-sensitive molecule that displays O-glycan-dependent binding activity. Moreover, the existence of a single peak distribution of rupture forces (Fig. 4b) suggests the presence of one major LS174T P-selectin ligand or, alternatively, the existence of more than one ligand with very similar properties.

In conclusion, we have employed single molecule force spectroscopy to probe *in situ* the biophysical parameters of P-selectin binding to ligands on intact human cells at the single molecule level. The differential abilities of PMNs and colon carcinomas to roll on P-selectin substrates are attributed in part to intrinsic differences in receptor/ligand binding affinity as well as varying densities of ligands on their respective cell surfaces. Given the

direct role of P-selectin in hematogenous spread (8, 9), characterizing the biochemical and biophysical properties of functional P-selectin ligands on carcinomas will provide guidelines to engineer novel therapeutic agents that will selectively block ligand function and thus interfere with metastatic spread. Such a strategy would offer specific anti-metastatic efficacy without impairing other important P-selectin-mediated pathophysiological processes. The *in situ* technique presented here provides a direct means for evaluating the efficacy of potential adhesion-blocking therapeutic agents.

Acknowledgments—We thank Dr. Ray Camphausen (Wyeth External Research) for the generous gift of P-selectin Fc IgG chimera protein. We also acknowledge fruitful discussions with Jason Cleveland (Asylum Research, Inc.) and with Dr. Ronald L. Schnaar (The Johns Hopkins University School of Medicine).

REFERENCES

- McEver, R. P. (2002) *Curr. Opin. Cell Biol.* **14**, 581–586
- Konstantopoulos, K., Kukreti, S., and McIntire, L. V. (1998) *Adv. Drug Deliv. Rev.* **33**, 141–164
- Springer, T. A. (1995) *Annu. Rev. Physiol.* **57**, 827–872
- Giavazzi, R., Foppolo, M., Dossi, R., and Remuzzi, A. (1993) *J. Clin. Invest.* **92**, 3038–3044
- Mannori, G., Crottet, P., Cecconi, O., Hanasaki, K., Aruffo, A., Nelson, R. M., Varki, A., and Bevilacqua, M. P. (1995) *Cancer Res.* **55**, 4425–4431
- Mannori, G., Santoro, D., Carter, L., Corless, C., Nelson, R. M., and Bevilacqua, M. P. (1997) *Am. J. Pathol.* **151**, 233–243
- Moore, K. L., Patel, K. D., Bruehl, R. E., Li, F., Johnson, D. A., Lichenstein, H. S., Cummings, R. D., Bainton, D. F., and McEver, R. P. (1995) *J. Cell Biol.* **128**, 661–671
- Borsig, L., Wong, R., Hynes, R. O., Varki, N. M., and Varki, A. (2002) *Proc. Natl. Acad. Sci. U. S. A.* **99**, 2193–2198
- Borsig, L., Wong, R., Feramisco, J., Nadeau, D. R., Varki, N. M., and Varki, A. (2001) *Proc. Natl. Acad. Sci. U. S. A.* **98**, 3352–3357
- McCarty, O. J., Mousa, S. A., Bray, P. F., and Konstantopoulos, K. (2000) *Blood* **96**, 1789–1797
- Goetz, D. J., Ding, H., Atkinson, W. J., Vachino, G., Camphausen, R. T., Cumming, D. A., and Lusinskas, F. W. (1996) *Am. J. Pathol.* **149**, 1661–1673
- Aigner, S., Ramos, C. L., Hafezi-Moghadam, A., Lawrence, M. B., Friederichs, J., Altevogt, P., and Ley, K. (1998) *FASEB J.* **12**, 1241–1251
- Alon, R., Hammer, D. A., and Springer, T. A. (1995) *Nature* **374**, 539–542
- Ramachandran, V., Yago, T., Epperson, T. K., Kobzdej, M. M., Nollert, M. U., Cummings, R. D., Zhu, C., and McEver, R. P. (2001) *Proc. Natl. Acad. Sci. U. S. A.* **98**, 10166–10171
- Park, E. Y., Smith, M. J., Stropp, E. S., Snapp, K. R., DiVietro, J. A., Walker, W. F., Schmidtko, D. W., Diamond, S. L., and Lawrence, M. B. (2002) *Biophys. J.* **82**, 1835–1847
- Fritz, J., Katopodis, A. G., Kolbinger, F., and Anselmetti, D. (1998) *Proc. Natl. Acad. Sci. U. S. A.* **95**, 12283–12288
- Goetz, D. J., Greif, D. M., Ding, H., Camphausen, R. T., Howes, S., Comess, K. M., Snapp, K. R., Kansas, G. S., and Lusinskas, F. W. (1997) *J. Cell Biol.* **137**, 509–519
- Kim, Y. J., Borsig, L., Han, H. L., Varki, N. M., and Varki, A. (1999) *Am. J. Pathol.* **155**, 461–472
- Capon, C., Wieruszkeski, J. M., Lemoine, J., Byrd, J. C., Leffler, H., and Kim, Y. S. (1997) *J. Biol. Chem.* **272**, 31957–31968
- Somers, W. S., Tang, J., Shaw, G. D., and Camphausen, R. T. (2000) *Cell* **103**, 467–479
- Jadhav, S., and Konstantopoulos, K. (2002) *Am. J. Physiol.* **283**, C1133–C1143
- Jadhav, S., Bochner, B. S., and Konstantopoulos, K. (2001) *J. Immunol.* **167**, 5986–5993
- Walcheck, B., Moore, K. L., McEver, R. P., and Kishimoto, T. K. (1996) *J. Clin. Invest.* **98**, 1081–1087
- Benoit, M., Gabriel, D., Gerisch, G., and Gaub, H. E. (2000) *Nat. Cell Biol.* **2**, 313–317
- Tees, D. F., Waugh, R. E., and Hammer, D. A. (2001) *Biophys. J.* **80**, 668–682
- Burdick, M. M., Bochner, B. S., Collins, B. E., Schnaar, R. L., and Konstantopoulos, K. (2001) *Biochem. Biophys. Res. Commun.* **284**, 42–49
- Chesla, S. E., Selvaraj, P., and Zhu, C. (1998) *Biophys. J.* **75**, 1553–1572
- Evans, E., Leung, A., Hammer, D., and Simon, S. (2001) *Proc. Natl. Acad. Sci. U. S. A.* **98**, 3784–3789
- Schweisinger, F., Ros, R., Strunz, T., Anselmetti, D., Guntherodt, H. J., Honegger, A., Jermutus, L., Tiefenauer, L., and Pluckthun, A. (2000) *Proc. Natl. Acad. Sci. U. S. A.* **97**, 9972–9977
- Strunz, T., Oroszlan, K., Schafer, R., and Guntherodt, H. J. (1999) *Proc. Natl. Acad. Sci. U. S. A.* **96**, 11277–11282
- Evans, E., and Ritchie, K. (1997) *Biophys. J.* **72**, 1541–1555
- Sheikh, S., and Nash, G. B. (1998) *J. Cell. Physiol.* **174**, 206–216
- Yarmola, E. G., Somasundaram, T., Boring, T. A., Spector, I., and Bubb, M. R. (2000) *J. Biol. Chem.* **275**, 28120–28127
- Smith, M. J., Berg, E. L., and Lawrence, M. B. (1999) *Biophys. J.* **77**, 3371–3383
- Mehta, P., Cummings, R. D., and McEver, R. P. (1998) *J. Biol. Chem.* **273**, 32506–32513